

Suppression of Alfvén modes through additional beam heating

N. Gorelenkov, E. D. Fredrickson, E. Belova, N. A. Crocker^a, B. LeBlanc, A. Diallo, M. Podestà, R. E. Bell, D. Darrow, D. Battaglia, S. Gerhardt

Princeton Plasma Physics Laboratory, Princeton New Jersey 08543

^aDepartment of Physics and Astronomy, University of California, Los Angeles, CA 90095

eric@pppl.gov

Abstract. The International Tokamak Experimental Reactor (ITER) will have a large population of non-thermal, energetic ions consisting of fusion generated alphas and beam ions injected for current profile control. Potential redistribution and/or loss of those non-thermal ions is thus of concern as it will modify heating profiles, current profiles, and losses could lead to unacceptable local heating of plasma facing components. Redistribution and losses of fast ions have been documented as resulting from multiple Alfvénic modes, Toroidal Alfvén Eigenmodes and energetic particle modes (fishbones) on many smaller plasma devices. This paper presents experimental evidence that some fast ion driven instabilities can be suppressed by modifying the fast-ion distribution function. The experimental results were modeled using the HYM code and provide a valuable validation of our theoretical understand of fast-ion-driven instabilities. ITER will necessarily have a large population of fusion-generated super-Alfvénic alphas, and like the beam ions in NSTX-U, these alphas will excite a variety of beam-driven instabilities. Neither NSTX-U, nor any other operating tokamak can simultaneously match all relevant fast-ion parameters to those expected for ITER, so predictions of fast-ion driven modes on ITER will rely on well-developed and validated theory. NSTX-U, which sees a broad spectrum of modes excited by the neutral beam ions, provides a laboratory to improve our understanding of this physics and to develop tools to control these instabilities, or to predict their affect on ITER.

1. Introduction

NSTX and now NSTX-U [1] routinely operate with a super-Alfvénic fast ion population. This non-thermal population heats the thermal plasma, and in some cases is used to control the current profile to enhance plasma stability. However, the non-thermal fast ions also excite a broad range of instabilities, including fishbones, Toroidal Alfvén eigenmodes (TAE), Compressional Alfvén eigenmodes (CAE) and in particular, Global Alfvén eigenmodes (GAE). Global Alfvén eigenmodes have been implicated in electron thermal transport and fast ion redistribution. In this paper we will show that the addition of more neutral beam power, can under the right circumstances, suppress the GAE.

2. Suppression of GAE

In Figure 1 is shown one of many examples where the addition of an appropriate neutral beam source suppresses an existing GAE. This is an 0.6MA target plasma with a nominal 0.65T toroidal field and two neutral beam sources injecting a total of 3.3 MW of heating power. The plasma density is peaked, with central density of $\approx 3.3 \times 10^{19}/\text{m}^3$ and the peak electron and ion temperatures are ≈ 1.7 keV. The core rotation frequency is ≈ 28 kHz. A spectrogram based on the toroidal Mirnov coil array data is shown in Fig. 1a. The toroidal mode numbers, are indicated by colors, with the dominant modes being $n=-10$ (green) and

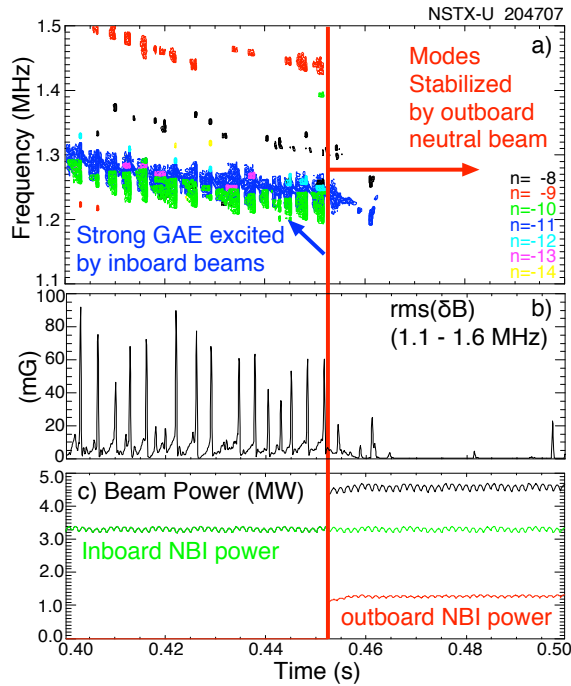


Fig. 1. a) color-coded spectrogram showing GAE activity. Dominant modes are $n=-10$ (green) and $n=-11$ (blue). b) RMS magnetic fluctuation amplitude over the frequency range 1.1-1.6 MHz, c) green curve is inboard beam power, red curve is off-axis beam power (source 2c).

The third neutral beam source adds only ≈ 1.3 MW of additional heating power; making up a little more than one fourth of the total NBI heating power after 0.45s. The suppression of GAE activity begins nearly simultaneously with the third source injection; on a timescale much shorter than the fast-ion slowing down time of 0.13 s - 0.16 s. By 0.46s, 10ms after outboard source injection started, the neutron rate, a measure of the confined fast ion population, has increased less than 7% with a 30% increase in beam power.

The new capability to control the fast ion distribution afforded by the new neutral beam sources on NSTX-U was key to demonstrating reliable suppression of the ctr-propagating Global Alfvén eigenmode (GAE). NSTX-U has six beam sources, the original three from NSTX with tangency radii inboard of the magnetic axis at $R_{\text{tan}} \approx 0.7, 0.6$ and 0.5m , (labeled 1a, 1b, 1c, respectively), and three new outboard sources with $R_{\text{tan}} = 1.3, 1.2$ and 1.1m (labeled 2a, 2b, 2c, respectively). A sketch of the neutral beam geometry is shown in Fig. 2. The red lines show the trajectories of the original, “inboard” neutral beam lines and the green lines show the trajectories of the new, “outboard”

$n=-11$ (blue). There are also weaker $n=-8, -9, -12$ and -13 modes. The modes are propagating counter to the beam injection, toroidal rotation and plasma current directions with a lab-frame frequency of ≈ 1.25 MHz at the analysis time of 0.44s. The counter-propagation is consistent with a model predicting a Doppler-shifted cyclotron resonance (in the resonant beam ion frame, the mode frequency is equal to the ion cyclotron frequency). Correcting for the plasma rotation frequency, the mode frequency in the plasma frame is ≈ 1.5 MHz or $\approx 0.4 \omega_{\text{ci}}$.

At 0.45s a third neutral beam source (2c) is injected (Fig. 1c, red curve), and the GAE are suppressed. The suppression of the GAE can be seen in Fig. 1a, and more clearly in Fig. 1b,

which shows the rms amplitude of the GAE

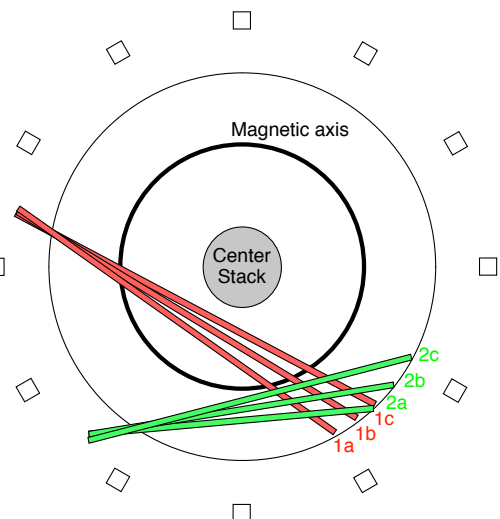


Fig. 2. Sketch of neutral beam geometry. Original NSTX beams in red, labeled 1a, 1b, 1c, new beams for NSTX-U shown in green labeled 2a, 2b and 2c.

neutral beam lines. The approximate magnetic axis location for this shot ($R_{\text{mag}} \approx 1.05$ m) is shown in black. All of the outboard neutral beams inject fast ions onto trajectories largely parallel to the magnetic field, thus with pitch, $0.8 < V_{\parallel}/V < 1$. It should be noted, however, that the fast ion distributions from sources 2b and 2c are still peaked on axis and only 2a creates a beam beta that is peaked off-axis.

The GAE have been implicated in enhancing electron energy transport, and there is indirect evidence that they affect the fast-ion distribution. In addition to the GAE, the neutral beams excite Toroidal Alfvén eigenmodes (TAE) at lower frequency. The spectrograms showing the GAE and the TAE on an expanded timescale are shown in Figs. 3a (GAE) and 3b (TAE). As has been reported previously, the GAE bursts appear to trigger the TAE avalanches. In Fig. 3c is shown the rms amplitude of the TAE (black) and the GAE (red). Three of the six strong TAE bursts are directly preceded by GAE bursts, providing indirect evidence that the GAE redistribute fast ions. The neutron rate is shown in Fig. 3d, and with each strong TAE avalanche, the neutron rate drops by $\approx 5\%$. The effects of the GAE and TAE are not incorporated in the calculations of the fast ion distributions discussed below, however, the short timescale needed for the outboard source to suppress the GAE suggests that there would be little time for modification of the distribution of fast ions injected from that source before the GAE were suppressed.

Estimates of the growth and damping rates for the GAE can be made from the growth and decay rates of the GAE bursts. The bursts last for about $70 \mu\text{s}$. The growth rate, γ_{growth} , of the burst is measured to be about $13 \mu\text{s}$ and the decay rate, $|\gamma_{\text{decay}}|$, is about $16 \mu\text{s}$. With the assumption that the damping rate is constant, and that the growth rate of the burst is $|\gamma_{\text{growth}}| \approx |\gamma_{\text{drive}}| - |\gamma_{\text{damp}}|$, and that $|\gamma_{\text{damp}}| \geq |\gamma_{\text{decay}}|$, then $\gamma_{\text{drive}} \geq |\gamma_{\text{growth}}| + |\gamma_{\text{decay}}|$. For comparison to the simulation results below, those numbers are normalized to the ion cyclotron frequency of $\approx 2.7 \times 10^7$ radians/s to get $\gamma_{\text{drive}}/\omega_{\text{ci}} \approx 0.5\%$.

The rapid suppression of the GAE is demonstrated more clearly in Fig. 4. In this shot a sequence of beam pulses with $\approx 3\text{ms}$ duration are injected every 16ms into a beam heated

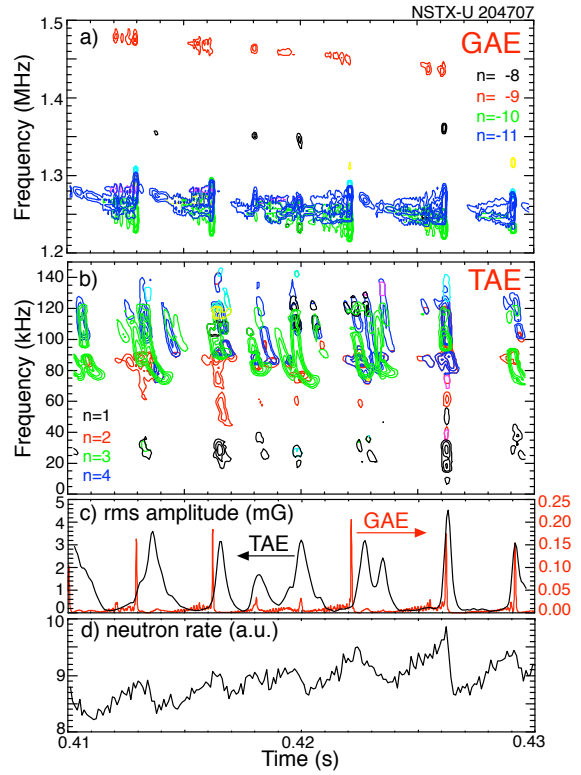


Fig. 3. a) color-coded spectrogram showing GAE activity. Dominant modes are $n=-10$ (green), $n=-11$ (blue), b) color-coded spectrogram showing TAE activity. Dominant modes are $n=2$ (red), $n=3$ (green) and $n=4$ (blue), c) rms amplitude of GAE (red) and TAE (black) on separate scales, d) neutron rate showing drops with each TAE burst.

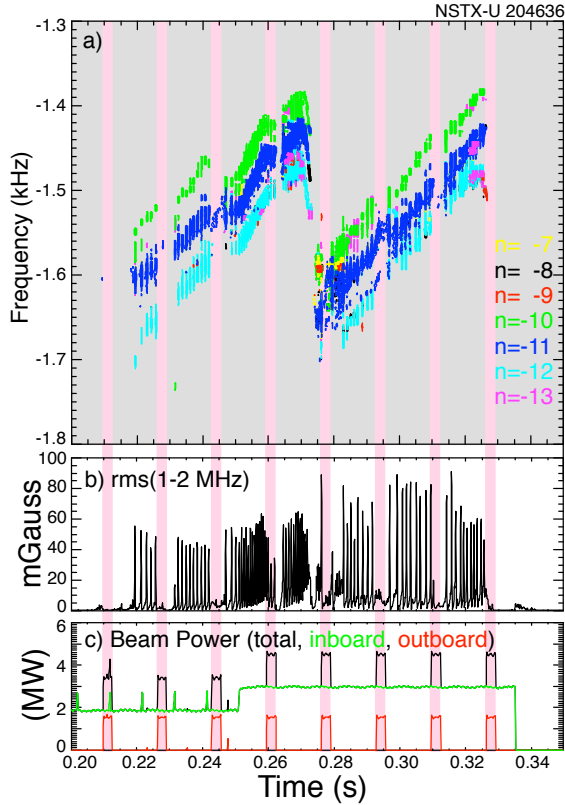


Fig. 4. a) color-coded spectrogram showing GAE activity. Dominant modes are $n=-10$ (green), $n=-11$ (blue), $n=-12$ (cyan), b) rms amplitude of GAE, pink bars indicate when outboard source is on, c) injected beam power, green is total inboard source power, red shows outboard beam pulses (source 2b).

two important changes in the fast ion distribution. The first is that there are substantially more fast ions with very high pitch, that is, with relatively little perpendicular energy and small larmor radii. The second is that the higher pitch fast ions added by the third neutral beam source, 2c, reverse the gradient in the pitch direction in the fast ion distribution. Both of these changes may be related to the suppression of the counter-propagating GAE.

The GAE are measured to be counter-propagating, which implies that the drive is through a Doppler-shifted cyclotron resonance, that is, that in the fast-ion frame the mode frequency is Doppler-shifted to match the cyclotron frequency;

$$\omega_{mode} + (k_{\parallel} \pm 1/qR)V_{b\parallel} = \omega_{ci} \quad \text{Eq. 1}$$

plasma with GAE activity. In Fig. 4a it is seen that the dominant modes are $n=-10$ (green), -11 (blue) and -12 (cyan). The pink bars indicate when the 3rd source is on. In Fig. 4b is shown the rms GAE amplitude showing bursting modes of comparable amplitude to those in Fig. 1. The bursts are completely suppressed with injection of the 3rd (outboard) source (Fig. 4c), with the exception of the fourth beam pulse during which there are two weaker GAE bursts. This clearly demonstrates that suppression can occur on a millisecond timescale and very few additional fast ions are needed to suppress the modes.

3. Theoretical analysis

The change in the fast ion distribution resulting from the addition of the third source is calculated with the TRANSP code and is shown in Fig. 5 at 0.44s (just before) and at 0.47s (just after). The third neutral beam adds resonant fast ions with pitches greater than ≈ 0.9 . There are

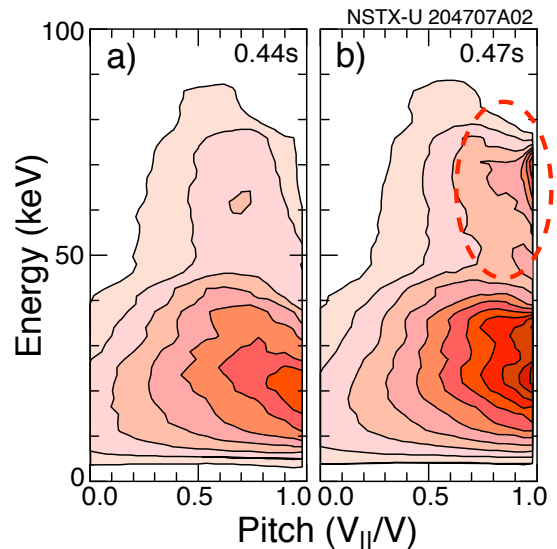


Fig. 5. TRANSP fast-ion distributions for before and after the outboard beam injection. The dashed oval indicates fast ions believed responsible for GAE suppression. Distribution functions are average over whole plasma volume. Contour spacing is linear, beginning at 1×10^7 up to $1.1 \times 10^8 / \text{cm}^3/\text{eV}/\text{dA}$.

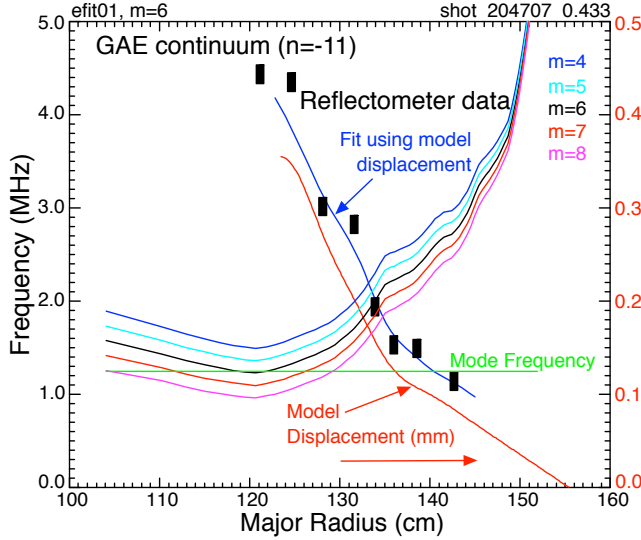


Fig. 6. Calculation of the GAE continuum for the $n=-11$ for $m=4-8$ modes ($\omega=|k_{||}V_{Alvén}-n\omega_{rot}|$). Indicated in green is the observed laboratory mode frequency. Overlaid are the reflectometer data (black rectangles), and modeled GAE displacement (red), simulated reflectometer response (blue). The mode frequency of 1.25 MHz (green), which points to $m \approx 6$, and the profile of the mode amplitude determined with a multichannel reflectometer array. The inferred mode amplitude, measured by the inferred displacement, peaks inside of $R \approx 1.24$, inside of which there are no reflecting reflectometer channels. This absolute amplitude and the amplitude profile of GAE are comparable to that reported on NSTX [2]. Using the inferred value of $m \approx 6$, from which we can calculate the radial profile of $k_{||}$, we can now estimate which fast ions might satisfy the resonance condition.

An analytic theory of GAE stability predicts drive and damping from fast ions as a function of the dimensionless parameter $k_{\perp}\rho$ [3], where ρ is the Larmor radius of the resonant energetic fast ion. The model predicts that for $k_{\perp}\rho < 1.9$, the resonant fast ions will be stabilizing, and destabilizing for $1.9 < k_{\perp}\rho < 3.9$. The minimum beam energy which can satisfy the resonance condition, corresponding to the resonant beam-ion parallel velocity, is shown in Fig. 7 (blue line) for the lower energy solution to the resonance condition in Eq. 1. The area in Fig. 7 colored light green (below the blue line) shows ions

where $V_{b||}$ is the parallel beam ion velocity. Matching this resonance condition puts constraints on the term $k_{||}V_{b||}$. To determine which fast ions might satisfy the resonance, we first evaluate the simple GAE dispersion relation;

$$\omega_{mode} = k_{||}V_{Alvén} + |n|\omega_{rotation} \quad \text{Eq. 2}$$

to find the magnitude of $k_{||}$, where $k_{||} = n/R - m/qR$. In Fig. 6 is shown the profile of the mode frequency for $m = 4$ through 8, and $n=-11$ (counter-propagating). The mode frequency profile has a minimum around $R = 1.2m$. Overlaid is the mode

frequency of 1.25 MHz (green), which points to $m \approx 6$, and the profile of the mode amplitude determined with a multichannel reflectometer array. The inferred mode amplitude, measured by the inferred displacement, peaks inside of $R \approx 1.24$, inside of which there are no reflecting reflectometer channels. This absolute amplitude and the amplitude profile of GAE are comparable to that reported on NSTX [2]. Using the inferred value of $m \approx 6$, from which we can calculate the radial profile of $k_{||}$, we can now estimate which fast ions might satisfy the resonance condition.

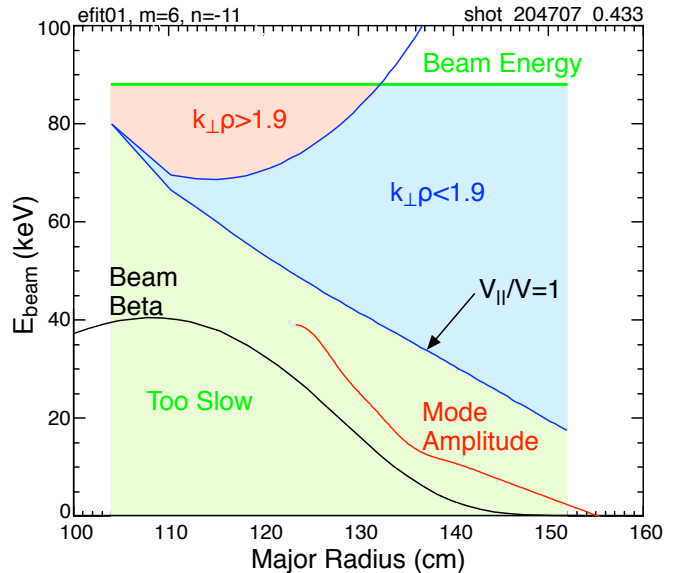


Fig. 7. Pictogram showing which beam ions are too slow to be resonant (green region), could be resonant and damping (blue region), and could be resonant and drive the ctr-GAE (red) regions. Also shown are the shape of the fast ion beta profile, showing highest fast ion beta (black line) within $R \approx 1.25m$, the shape of the measured mode amplitude (red line), peaking inside 1.25 m and maximum beam injection energy of ≈ 88 keV.

that are too slow to be resonant with the modes. The areas colored blue or pink above the blue line show fast ions with energies sufficiently high to be resonant with the mode, and the further from the blue line, corresponding to $V_{||}/V = 1$, the lower the pitch of the resonant beam-ions. Also shown is the profile of β_{fast} (black line) and the radial profile of the mode amplitude (red line) showing that the most important region of the figure is probably inside roughly $R < 1.3m$. The area colored pink in Fig. 7 shows fast ions which have high enough energy to satisfy the parallel resonance condition, and still have enough perpendicular energy to satisfy $k_{\perp}\rho_L > 1.9$. These calculations contain many approximations, including the use of a q profile from EFIT that wasn't constrained by MSE data.

The cyclotron resonance means that modeling mode stability requires a code which uses a full orbit beam-ion model. The HYM code [4] is an initial value, hybrid code in toroidal geometry which treats the beam ions using a full-orbit, delta-f particle simulation. The background plasma is represented by a one-fluid resistive MHD model. The distribution function is input to the code in an analytic form. The example of GAE suppression shown in Fig. 1 has been modeled using simulations with the HYM code using reconstructed equilibria and the fast ion parameters as calculated in the TRANSP code. The fast ion distribution function is based on an 'ideal' calculation which doesn't consider modifications to the distribution from the strong TAE avalanching present throughout the beam heating phase.

HYM has accurately predicted the most unstable modes and the mode frequencies (not including the Doppler correction). Using plasma equilibrium parameters and the fast-ion distribution function calculated at 0.44s, before the modes were suppressed, the HYM code finds unstable GAE with $n=-7$ through -12 (Fig. 8a). The linear growth rates for the modes are shown in Fig. 8a, with the fastest growing mode being $n=-10$, in good agreement with the experimental measurements. The mode frequencies are shown in Fig. 8b (red curve). HYM doesn't include the toroidal rotation, so an approximate Doppler correction is made to the simulated mode frequencies (blue curve) and which are in good agreement with the experimental frequencies (blue *). The polarization of the magnetic fluctuations shows that the modes have shear polarization near the peak in mode amplitude, showing that the modes found by HYM are in fact GAE and not Compressional Alfvén eigenmodes.

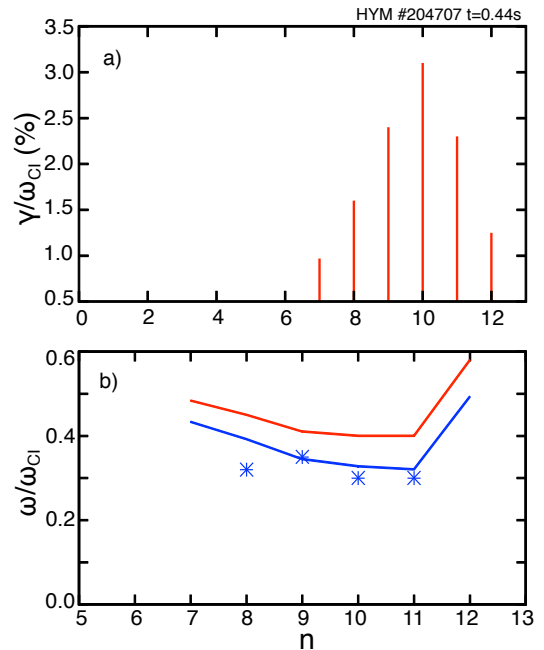


Fig. 8. (a) Growth rates and (b) frequencies of unstable counter-GAEs from HYM simulations for $t=0.44s$. Blue line is Doppler-shift corrected frequencies, points – experimental values.

In Fig. 9 are compared the growth of the $n=-10$ GAE at the time from before the injection of the outboard source (0.44s, red curve) and the growth of the $n=-10$ eigenmode using the equilibrium and fast-ion distribution function from 0.47s, approximately 20 ms after the start of injection of the third beam source (blue curve). As can be seen in Fig. 9, the $n=-10$ mode is stabilized with the injection of the outboard beam source. Further HYM runs have so far found that the modes with $n=-7$ to -11 modes were also stable.

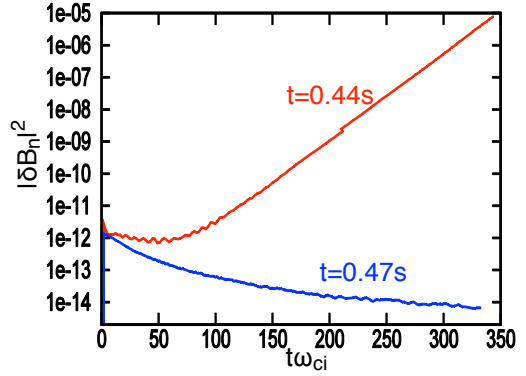


Fig. 9. Time evolution of magnetic energy of $n=10$ GAE from HYM simulations for $t=0.44$ s (red) and $t=0.47$ s (blue). $n=10$ GAE is suppressed with additional beam power.

3. Summary

The recently completed upgrade to NSTX, NSTX-U, has doubled the number of beam sources from three sources to six. The new sources have tangency radii outside of the magnetic axis allowing much greater flexibility in generating the fast ion distribution. This flexibility has paid off in the first operational campaign on NSTX-U where it was found that the new beam sources were very effective at suppressing GAE, one of the common beam driven instabilities seen on NSTX, an instability that is correlated with enhanced core electron transport. Analysis of one of these NSTX-U discharges with the HYM code at a time during strong GAE activity find that the $n = -10$ and $n = -11$ ctr-propagating GAE are most unstable, in good agreement with experimental measurements. HYM predicts that the GAE have strong growth rates of 2-3% of the ion-cyclotron frequency. The experimental growth rates are difficult to measure, but appear to be significantly smaller ($\approx 0.5\% \omega_{ci}$), possibly because the distribution function used in HYM is unperturbed. The predicted Doppler-corrected mode frequencies are between $0.3 \omega_{ci}$ and $0.35 \omega_{ci}$, in very good agreement with the observed mode frequencies. HYM simulations using the TRANSP fast-ion distribution functions which include one of the new beam sources find that the $n = -7$ and -11 modes become stable (*cf.* Fig 9 for mode energy evolution of the $n = -10$ mode, red before, blue after). These results suggest that stabilization may be due to a change in the slope of distribution function. A second explanation is a model where the drive and damping from fast ions is stabilizing for $k_{\perp}\rho_L < 1.9$, and destabilizing for $1.9 < k_{\perp}\rho_L < 3.9$ [3]. The outboard neutral beams inject nearly tangential fast ions, which have relatively smaller ρ_L than the fast ions from the inboard beams. Further work is required to improve understanding of the suppression mechanism. The agreement between theory and experiment in these initial results from the HYM code with the experimental measurements provide a strong validation of the HYM code physics.

Work supported by U.S. DOE Contract DE-AC02-76CH03073 and DE-FG02-99ER54527.

Appendix:

- [1] M. Ono, S. M. Kaye, Y.-K. M. Peng, *et al.*, Nucl. Fusion **40**, 557 (2000).
- [2] N. A. Crocker, E. D. Fredrickson, N. N. Gorelenkov, W. A. Peebles, S. Kubota, R. E. Bell, A. Diallo, B. P. LeBlanc, J. E. Menard, M. Podestà, K. Tritz, H. Yuh, *et al.*, Nucl. Fusion **53** (2013) 043017.
- [3] N.N. Gorelenkov, E. Fredrickson, E. Belova, C.Z. Cheng, D. Gates, S. Kaye and R. White, Nucl. Fusion **43** (2003) 228.
- [4] E. V. Belova,^a) N. N. Gorelenkov, and C. Z. Cheng, Phys. Plasmas **10** (2003) 3240.